Modeling of the sub-T_g relaxation spectrum of $Pd_{42.5}Ni_{7.5}Cu_{30}P_{20}$ metallic glass.

Chaoren Liu[a], *Eloi Pineda*[b,*], *Jichao Qiao*[c], *Daniel Crespo*[a]

[a] Departament de Física, Universitat Politècnica Catalunya - BarcelonaTech, EETAC, Esteve Terradas 5, 08860 Castelldefels, Spain.

chaorenliu@gmail.com / daniel.crespo@upc.edu

[b] Departament de Física, Universitat Politècnica Catalunya - BarcelonaTech, ESAB, Esteve Terradas 8, 08860 Castelldefels, Spain.

eloi.pineda@upc.edu

[c] School of Mechanics, Civil Engineering and Architecture, Northwestern Polytechnical University, Xi'an 710072, P.R. China

Keywords: Alpha relaxation, Beta relaxation, Mechanical spectroscopy, Metallic glasses

Abstract: In this work we study the mechanical relaxation spectrum of $Pd_{42.5}Ni_{7.5}Cu_{30}P_{20}$ metallic glass. The effect of aging on the relaxation behavior is analyzed by measuring the internal friction during consecutive heating runs. The mechanical relaxation of the well-annealed glass state is modeled by fitting susceptibility functions to the primary and secondary relaxations of the system. The model is able to reproduce the mechanical relaxation spectrum below the glass transition temperature (sub-T_g) in the frequency-

temperature ranges relevant for the high temperature physical properties and forming ability of metallic glasses. The model reveals a relaxation spectrum composed by the overlapping of primary and secondary processes covering a wide domain of times but with a relatively narrow range of activation energies.

INTRODUCTION

The mechanical relaxation behavior of metallic glasses is strongly related to the plastic and viscous deformation mechanisms as well as to the physical aging process. The microscopic mechanisms allowing the glassy structure to relax under an external mechanical perturbation must be similar to those involved in plasticity and viscous flow under continuous deformation. In addition, they are expected to be closely linked to those changing the glass structure towards more stable states during physical aging, as this process is driven by the release of internal stresses quenched-in during the glass formation process.

Mechanical relaxation of metallic glasses can be probed by quasi-static or by oscillatory measurements. In quasi-static measurements, a constant stress σ_0 (or strain ε_0) is 'instantaneously' applied and the time evolution of strain $\varepsilon(t)$ (or stress $\sigma(t)$) is characterized by a response function $\varphi(t)$ which usually has the look of a stretched exponential decay. In oscillatory measurements, the ratio between stress and strain is given by the complex elastic modulus $M(\omega)=M'(\omega)+iM''(\omega)$ composed by the storage (M') and loss (M'') moduli and determined by a frequency-domain response function $\chi(\omega)$[1]. The general form of the complex modulus obtained by mechanical spectroscopy is

$$M(\omega,T)=M_0(T)-\Delta M_\alpha\chi_\alpha(\omega,T)-\Delta M_\beta\chi_\beta(\omega,T)-\ldots \qquad (1)$$

where M_0 is the high-frequency limit modulus while ΔM_i and $\chi_i(\omega,T)$ are the intensity and the frequency-domain response function of the different relaxation processes present in the material. M_0 and ΔM_i are real magnitudes while $\chi_i(\omega,T)=\chi_i'(\omega,T)-i\chi_i''(\omega,T)$ determines the shape of both the storage modulus decay and the loss modulus peak. M corresponds to the Young's, shear or bulk modulus depending on the loading mode used in the experiment. The complex modulus behavior can be characterized by fixing the frequency while scanning temperature (isochronal measurements) or by fixing the temperature while scanning frequency (isothermal measurements).

The mechanical relaxation spectrum, $M''(\omega,T)$, of Pd-based metallic glasses was recently characterized by Qiao et al.[2,3]. As expected, the elastic-solid/viscous-liquid transition was governed by the α-relaxation with a main relaxation time $\tau_\alpha(T)$ following a Vogel-Fulcher-Tamman[4–7] (VFT) behavior at temperatures above the glass transition temperature T_g. The shape of the response function $\chi_\alpha(\omega,T)$

$$\chi_\alpha(\omega,T)=\int_0^\infty\left[-\frac{d\varphi_\alpha(t,T)}{dt}\right]\exp(-i\omega t)dt \qquad (2)$$

was found consistent with a Kohlrausch-Williams-Watts (KWW) stretched exponential relaxation in the time domain[8]

$$\varphi_\alpha(t,T)=\exp\left[-(t/\tau_\alpha(T))^{\beta_{KWW}}\right]. \qquad (3)$$

Many different metallic glasses have been characterized by mechanical spectroscopy. Although different values of β_{KWW} are reported depending on the experimental technique or the relaxation state of the glass[9], the survey of the experimental data evidences that metallic glasses show a stretching exponent β_{KWW} ~0.5 independently of compositional or liquid fragility differences[8,10].

In the case of Pd-based metallic glasses, the relaxation peak shows an obvious shoulder at lower temperatures (for isochronal measurements) or, equivalently, at higher frequencies (for isothermal measurements). This shoulder is associated with a secondary process (β-relaxation) and, although with different degrees of intensity, was observed in all Pd-based alloys[3]. The presence of secondary relaxations has been found in many other metallic glasses[11,12]. In some systems, particularly La-based glasses, a distinguishable secondary relaxation is observed well separated from the α-peak[13–15]. In these latter cases the analysis of the two processes can be performed more easily, allowing one to determine both the shape of the response function $\chi_\beta(\omega,T)$ as well as the temperature dependence of the corresponding relaxation time $\tau_\beta(T)$. In other glassy systems, for instance Cu-Zr-based glasses, only an excess wing of the α-process is detected at temperatures below the glass transition[16]. The characterization of the secondary process in these systems is harder as it is almost completely overlapped with the α-peak tail generated when $\tau_\alpha(T)$ changes form liquid (VFT) to glassy (Arrhenius) behavior at $T < T_g$ [9,17].

In Pd-based metallic glasses the secondary process is partially overlapped with the main α-relaxation. This allows one the determination of many of its characteristics, particularly in the highest frequency region, but in the overlapping region the contributions of both processes are difficult to discriminate. Qiao et al. showed this clearly in figure 10b of ref. [2] where the superposition of the two relaxation models proposed for the α and β processes does not reproduce the intermediate region. The aim of this work is to obtain explicit relaxation functions able to model the relaxation spectrum $M''(\omega,T)$ of $Pd_{42.5}Ni_{7.5}Cu_{30}P_{20}$ metallic glass between room temperature and the glass transition, and relaxation times

ranging from hours to seconds. This temperature-time window comprises most of the mechanical tests as well as cold-working and forming processes applied to metallic glasses.

The $Pd_{42.5}Ni_{7.5}Cu_{30}P_{20}$ system is one of the most studied metallic glasses due to its outstanding stability against crystallization and excellent glass forming ability (GFA). It is chosen here as a representative of the Pd-based glasses showing partial overlapping between α and β relaxations based on previous dynamic mechanical analysis (DMA) experiments. The change of the relaxation spectrum due to physical aging is examined by exploring the loss modulus and the viscosity of different relaxation states. This allows us to discriminate the effect of *in situ* physical aging on the internal friction of the glass, as well as to compare the activation energy of viscous flow and mechanical relaxation in the glassy state. Finally, the current understanding of the nature of α and β relaxations is discussed and assessed considering the presented results.

EXPERIMENTAL METHODS

The rapidly-quenched ribbons were prepared by melt spinning of bulk samples of $Pd_{42.5}Ni_{7.5}Cu_{30}P_{20}$ under argon atmosphere. The copper wheel linear velocity was set at 40 m/s, obtaining amorphous ribbons of 30±5 μm and an estimated cooling rate of $10^{5\text{-}6}$ K/s during the quenching process. The amorphous character of the samples was confirmed by X-ray diffraction in a Bruker D8 Advance apparatus with Cu-K_α radiation. Differential scanning calorimetry (DSC) was performed using a NETZSCH 404 F3 equipment. The onset of the glass transition was detected in the range going from 553 to 567 K when applying constant heating rates from 2 K/min to 20 K/min. The onset of crystallization was detected at 620 K (at 2 K/min) and 650 K (at 20 K/min). The span between glass transition and crystallization was always larger than 60 K, as expected for this high-GFA alloy. The

dynamic mechanical analysis and elongation measurements were performed with a TA Instruments Q800 DMA in tension mode. The DMA measurements were recorded by applying oscillation amplitudes of 5 μm (equivalent to a strain of 0.05%).

RESULTS. A) EXPERIMENTAL MEASUREMENTS

Figure 1 shows the loss modulus $M''(\omega,T)$ measured at constant frequency $\omega/2\pi$ =1 Hz during consecutive 2 K/min heating ramps. The thermal protocol applied to the samples is shown in the inset of the figure; the final temperatures of the consecutive runs were set at 420, 470, 520, 570 and 585 K, respectively. As shown in the figure, the *in situ* physical aging during the annealing treatments is clearly reflected in a progressive diminution of the loss modulus and, consequently, of the internal friction. As expected from previous studies on metallic glasses[18] the background of the loss modulus at T < 400 K is progressively reduced due to physical aging. Furthermore, the shoulder of the relaxation peak, associated with the secondary relaxation process, is progressively reduced and shifted towards higher temperatures. The last run is performed after reaching a temperature above the calorimetric glass transition region in the previous one, although the sample is then well relaxed it still shows an evident shoulder overlapped with the low-temperature tail of the main α-relaxation. Further annealing does not produce significant changes in the mechanical relaxation spectrum.

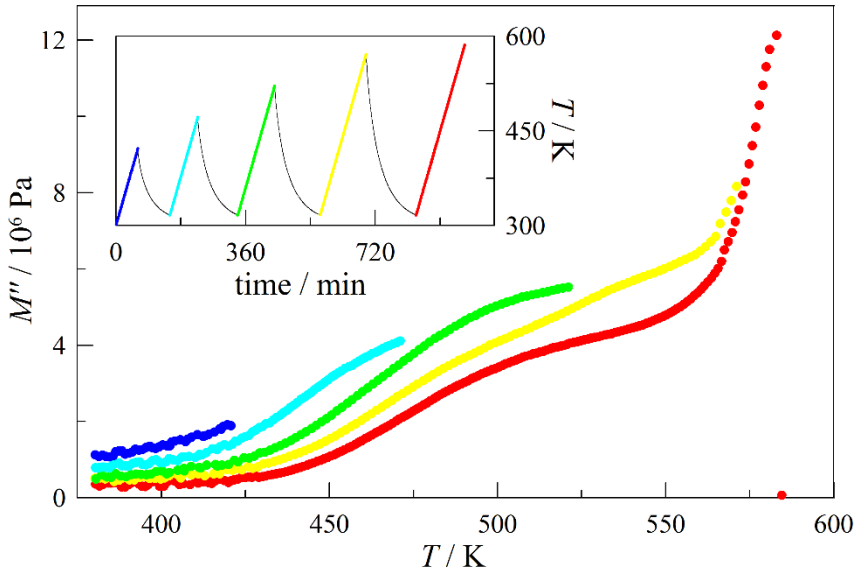

Figure 1. Loss modulus measured at a constant frequency of 1 Hz during consecutive heating runs. Inset: Thermal protocol applied to the samples. Different colors correspond to the corresponding consecutive heating runs.

Figure 2 shows the viscosity measured during the same thermal protocol. The shear viscosity was calculated from the measurement of the longitudinal viscosity as $\eta = \sigma/3\dot{\varepsilon}$ applying a constant static tensile force of 0.8 N and correcting the parasitic thermal expansion contribution of the equipment. The estimated error in the strain rate measurement is below 10^{-3} s^{-1}. The low stress applied during these measurements results in very low strain rates, thus assuring that the error induced by the reduction of the cross section of the ribbons is not significant until temperatures above 580 K. The right axis shows the corresponding relaxation times for viscous flow estimated as $\tau = \eta/G_0$ with G_0 = 30 GPa, which is the shear modulus expected for Pd-Ni-Cu-P amorphous alloys. As described in detail by Khonik et al.[19,20] the viscosity below T_g is dependent on the heating rate of the measurement as $\log\eta(T,\dot{T}) = f(T) - \log\dot{T}$; a shift due to the heating rate is also

expected for the internal friction DMA measurements[21,22]. In this work all DMA and elongation measurements were performed at the same 2 K/min heating rate.

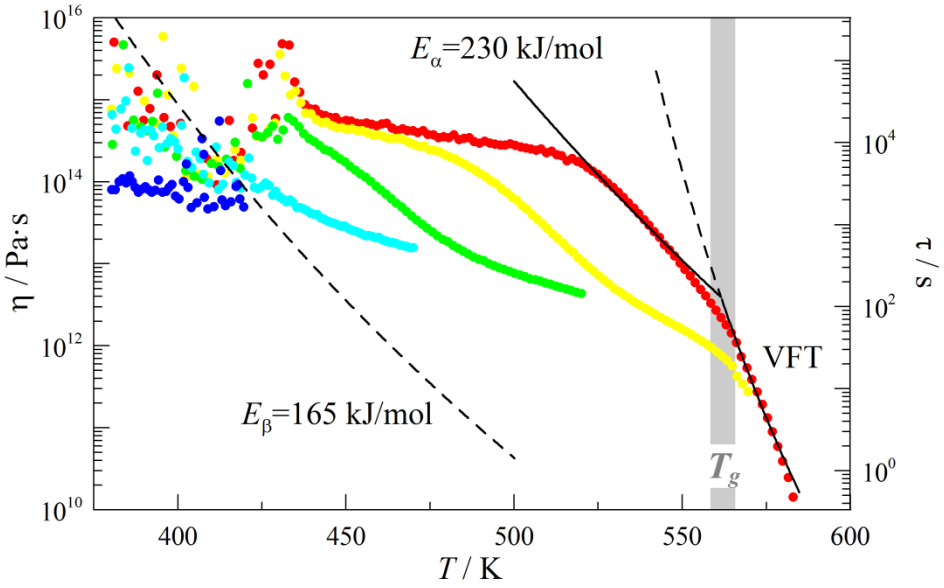

Figure 2. Viscosity measured at consecutive heating runs with the same annealing protocol as detailed in figure 1. Different colors correspond to the corresponding consecutive heating runs. Lines correspond to the average relaxation-time vs temperature behaviors $\tau_\alpha(T)$ (solid line) and $\tau_\beta(T)$ (dashed line) proposed in the model (see below). The $\tau_\alpha(T)$ changes from a VFT to Arrhenius behaviors at the liquid/glass transition, the extrapolation of the VFT behavior in the glass region is also depicted with a dashed line. Grey zone indicates the calorimetric glass transition region at the applied 2 K/min heating rate.

The effect of aging is clearly visible in the elongation behavior; the difference in viscosity between as-quenched and annealed ribbons is higher than one order of magnitude. The red line corresponds to relaxed ribbons (pre-annealed above glass transition) and it shows three different flow regions; below 525 K, between 525 K and T_g, and above T_g. In the low temperature region the viscosity is very high and diminishes slightly with increasing temperature, in this region the viscosity obtained from quasi-static creep

measurements is in well agreement with the one measured by monitoring elongation under continuous heating[23]. Above 525 K the viscosity decreases more rapidly with temperature, showing the expected change from glassy to liquid behavior at the glass transition region. Above T_g viscosity agrees well with the VFT behavior (solid line) calculated from the α-peak temperature position or from the liquid fragility as discussed below.

Relaxed ribbons, heated up to 573 K (above the glass transition) and cooled down to 313 K were subsequently analyzed by DMA. Both heating and cooling rates were set to 2 K/min. With this pre-annealing protocol the isochronal measurement at 2 K/min is expected to show the response of an isoconfigurational state with very small contribution of *in situ* physical aging while in the glassy state. Defining T_g as the calorimetric glass transition temperature detected at the same heating rate, the studied temperature range can be divided into two regions; one corresponding to an equilibrated supercooled liquid ($T > T_g$), the other corresponding to a glassy state ($T < T_g$). In the latter region the system is congealed in an out-of-equilibrium configuration with the applied heating rate fast enough to avoid equilibration. Isochronal measurements of $M'(\omega,T)$ and $M''(\omega,T)$ of relaxed ribbons performed at different frequencies are shown in figure 3. The dynamic glass transition detected at the different frequencies is clearly observed by the decay of the storage modulus and the main α-peak of the loss modulus. The dynamic glass transition for the range of frequencies studied occurs clearly above the calorimetric glass transition region.

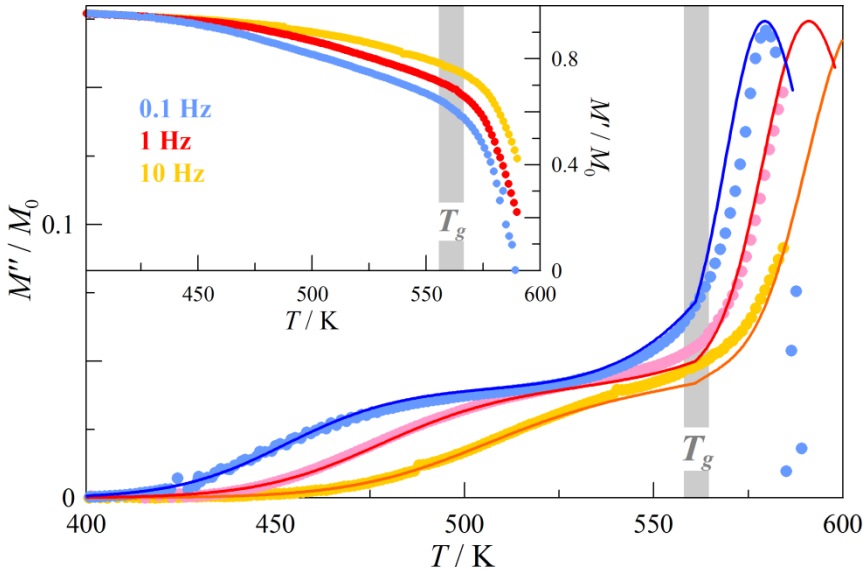

Figure 3. Isochronal measurements of loss modulus at 0.1, 1 and 10 Hz, respectively. The measurements were performed at constant 2 K/min heating rate. The samples were previously pre-annealed above T_g in order to avoid *in situ* physical aging during the measurements. Solid lines correspond to the model proposed in this work (see below). Inset shows the measurements of storage modulus. Grey zone indicates the calorimetric glass transition region at the applied 2 K/min heating rate.

RESULTS. B) MODELING OF PRIMARY AND SECONDARY RELAXATIONS

Similarly to previous works[24], the model is based on two relaxation processes (α and β). The modeling is performed for an isoconfigurational glass, i.e. it does not suffer *in situ* physical aging during the isochronal DMA measurements. Therefore, at temperatures below the glass transition the system is considered to be arrested in a one particular glassy state. For this isoconfigurational state the average relaxation times of the α and β processes, $\tau_\alpha(T)$ and $\tau_\beta(T)$, will be assumed to follow an Arrhenius behavior

$$\tau_\alpha(T) = \tau_{\alpha,0} \exp\left(\frac{E_\alpha}{RT}\right)$$
$$\tau_\beta(T) = \tau_{\beta,0} \exp\left(\frac{E_\beta}{RT}\right), \quad T < T_g \tag{4}$$

determined by the pre-exponential factors $\tau_{i,0}$ and the activation energies E_i. As already noted above, the assumption of an Arrhenius-like behavior for the sub-T_g α-relaxation is only valid if the glass structure is not changing during the experimental probe[1,25,26]. The Arrhenius behavior of isoconfigurational viscosity of metallic glasses was already described by Taub and Spaepen[27,28].

When the temperature is above T_g, the relaxation time of the α-process is assumed to follow a VFT function[1,29]

$$\tau_\alpha(T) = \tau_{\alpha,0}^{liq} \exp\left(\frac{B}{T - T_0}\right), \quad T > T_g \tag{5}$$

characterized by the empirical parameters $\tau_{\alpha,0}^{liq}$, B and T_0. The local $\tau_\alpha(T)$ behavior within a narrower temperature range at $T \gtrsim T_g$ can also be described by a fragility parameter, m, or an apparent activation energy, E_α^{liq}, which are then related to the VFT parameters by

$$m = \left.\frac{d \log \tau_\alpha}{d\, T_g / T}\right|_{T=T_g} = \frac{B T_g}{(T_g - T_0)^2 \ln 10} = \frac{E_\alpha^{liq}}{R T_g \ln 10}, \quad T \gtrsim T_g . \tag{6}$$

Here it must be noted that E_α^{liq} is linked to the fragility of the equilibrated liquid by equation 6 and therefore it is unique for a given substance. On the contrary, the activation energy E_α in equation 4 is specific of a given glassy configuration and may change with the thermal history of the sample. In other words, the supercooled liquid above T_g is in internal equilibrium and shows a unique $\tau_\alpha(T)$ equation while the relaxation time behavior in the glassy state is dependent on the particular glass configuration. The merging of the α

and β processes at temperatures above T_g is modeled by assuming that the dynamics of the secondary process changes progressively from Arrhenius to VFT behavior at $T > T_g$, both processes merging at the dynamic glass transition.

It is well known that the amorphous structure of liquids and glasses generates a broad distribution of activation energies for structural rearrangements and, consequently, of relaxation times. In this sense, it is important to clarify that equations 4 and 5 determine only the temperature dependence of the average relaxation times; the effect of the relaxation-time distributions around these average values is taken into account by the shape of the response functions $\chi_\alpha(\omega, \tau_\alpha(T))$ and $\chi_\beta(\omega, \tau_\beta(T))$ as discussed below.

The activation energies governing the behaviors described in equations 4 and 5 are determined by different means. The glass transition temperature is fixed at T_g =560 K, this corresponds to the inflection point of the calorimetric glass transition signal detected when applying a 2 K/min heating rate. The VFT function parameters are fitted from the positions of the α-peak maxima at different frequencies obtaining B =4400±10 K, T_0 =436±1 K and $\tau_{\alpha,0}^{liq}$ =8.2±0.3×10^{-14} s. These values produce a fragility parameter m =69 and an apparent activation energy E_α^{liq} =744 kJ/mol when evaluated at T_g =560 K. The values of fragility and VFT parameters are in good agreement with the ones obtained for Pd-Ni-Cu-P glassy alloys[3,30]. The activation energy of the β-relaxation, E_β, is obtained assuming that the two extremes of the frequency spectrum show only the contribution of one of the processes. In this case the time-temperature superposition (TTS) principle can be applied; if the process is controlled by an activation energy, the measurements at different frequencies converge in a master curve when shifted by the factor $E_{act}/RT\ln 10$ in a log-log plot. Figure 4 shows

the α and β regions of the loss modulus at different frequencies joined into master curves when shifted using E_α^{liq}=744 kJ/mol (determined from the VFT parameters) and E_β=165 kJ/mol (determined using the TTS principle). Finally, E_α, which defines the sub-T_g $\tau_\alpha(T)$ behavior in the overlapping region, is approached to be 230 kJ/mol from the viscosity measurements shown in figure 2.

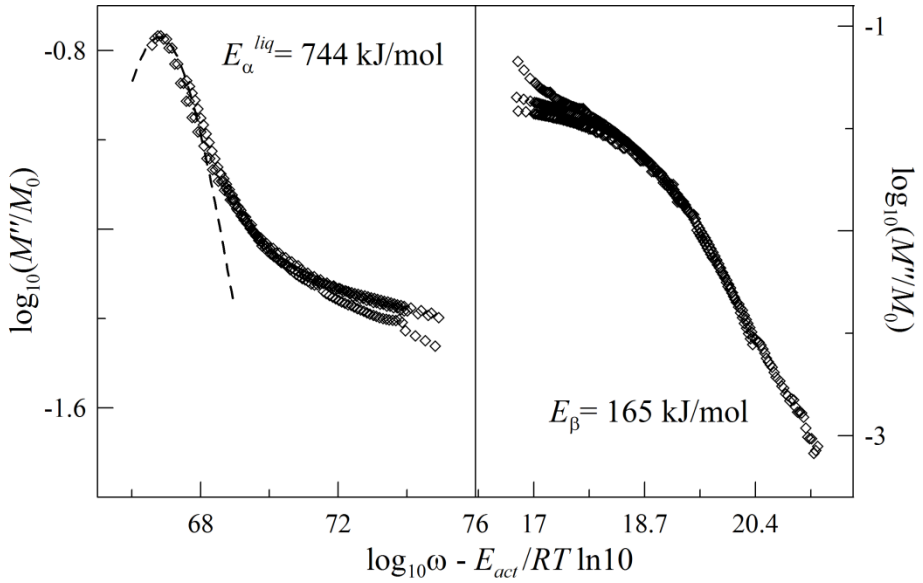

Figure 4. Log-log plots of the α-region (left) and the β-region (right) of the loss modulus shifted by the corresponding activation energies E_α^{liq} and E_β. The dashed line corresponds to a CC-function with broadening parameter α=0.5.

Two $\chi_\alpha(\omega,\tau_\alpha(T))$ and $\chi_\beta(\omega,\tau_\beta(T))$ response functions will be proposed here to describe the α and β relaxations. For the α-process the response of the system will be approximated by a Cole-Cole (CC) function[31]

$$\chi_\alpha(\omega,T)=\frac{1}{1+(i\omega\tau_\alpha(T))^\alpha}. \qquad (7)$$

Here it should be noticed that subscripts refer to the α-process while exponent α is the broadening parameter of the function. The imaginary part $\chi''_{\alpha}(\omega,T)$ of the CC-function gives a symmetric peak respect to $\log\omega$ and it is only able to reproduce the low-temperature (or high-frequency) side of the α-relaxation of metallic glasses[8]; in order to reproduce the whole shape an asymmetric function like Havriliak-Negami function[32] or the direct Fourier transform of the KWW function (equation 2) would have to be considered. As the aim of this work is to model the low-temperature (high-frequency) side region of the main relaxation, particularly the overlapping with the secondary relaxation, the use of the one-parameter CC-function is chosen in order to reduce the complexity of the model. In such sense, the important feature is that the decay of the high-frequency side coincides with the Fourier transform of the KWW function ($\varphi_{\alpha}(t,T)$ of equation 3) if $\alpha=\beta_{KWW}$ [33,34]. Following ref. [8,10] a value of $\alpha=\beta_{KWW}$ =0.5 will be assumed for the α-relaxation and its intensity is adjusted to $\Delta M_{\alpha}=0.8M_0$.

After subtracting the α-relaxation modeled by equations 4, 5 and 7 with the parameters specified just above, the experimental secondary relaxation is shown in figure 5. The shape of the secondary process corresponds to a broad and blunt peak with an intensity $\Delta M_{\beta}=0.2M_0$. The use of Havriliak-Negami (HN), Cole-Davidson (CD) or CC functions is not able to describe the bluntness of the experimental peak. For this reason a more general Bergman function[35]

$$\chi''_{\beta}(\omega,T)=\frac{p}{\frac{1-C}{a+b}\left[b(\omega\tau(T))^{-a}+a(\omega\tau(T))^{b}\right]+C} \tag{8}$$

is chosen to model the shape of the secondary process. A discussion of the basic traits of the diverse response functions used in the study of the relaxation phenomena in amorphous

substances is given in refs. [33,35]; for the Bergman function parameters a and b determine respectively the slope of the low and high-frequency tails, parameter C sets the bluntness of the peak and parameter p is used to adjust the height of the relaxation peak. Figure 5 shows the best fitting of the Bergman function given by a =0.58, b =0.67, p=0.18 and C =0.86.

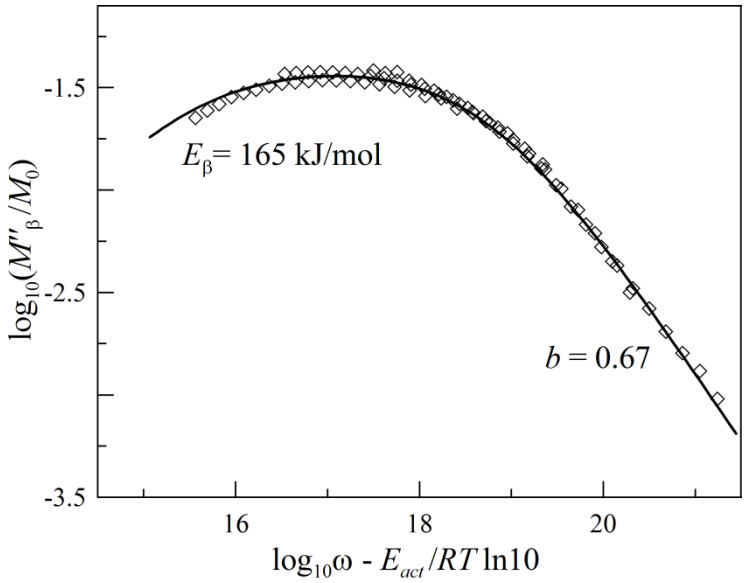

Figure 5. Symbols; Experimental M'' after subtracting the contribution of M''_α modeled by equations 4, 5 and 7. Line; The fitted Bergman function used to model the secondary relaxation M''_β.

The result of the model proposed for $M''(\omega,T)$ adding the contribution of the two relaxation processes is depicted by continues lines and compared with experimental data (symbols) in figure 3 above. The explicit contribution of the two relaxation functions and the reproduction of the experimental overall behavior for the case of 1 Hz are shown in figure 6. In next section the validity and reasonableness of the approaches used in the modeling will be discussed, here it is noticed that the experimental data is well-described

within the frequency and temperature range usually probed by mechanical spectroscopy of metallic glasses.

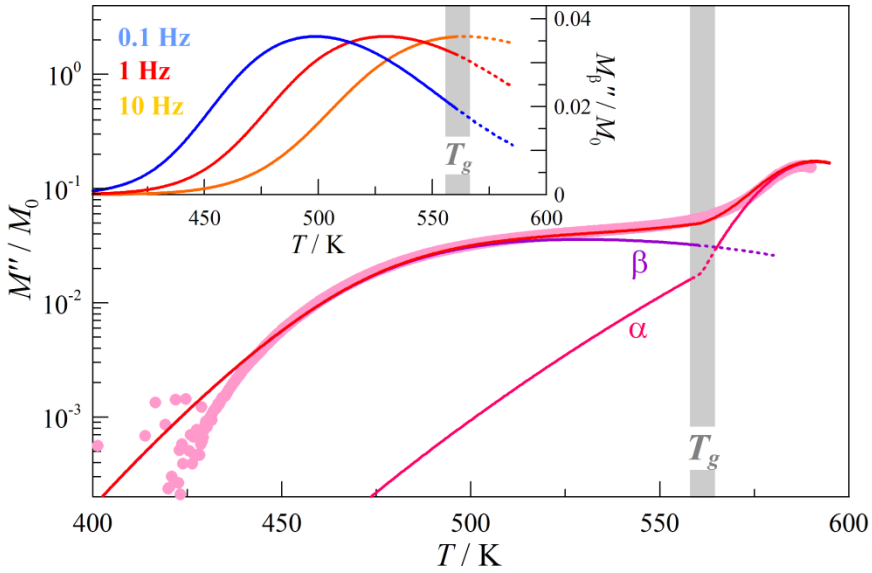

Figure 6. Experimental loss modulus at 1 Hz (symbols) compared with the results of the model (lines). The contributions of each process are depicted for further discussion. Inset shows the secondary process as modeled by a Bergman function and an Arrhenius temperature-dependence of the average relaxation time.

DISCUSSION

The effect of physical aging, as seen in figures 1 and 2, is huge on both loss modulus and viscosity. Considering the two figures, it is clear that the higher loss modulus observed in the first heating-cooling cycles coincides in temperature with physical aging driving the system towards states of higher viscosity. This implies that the physical aging occurring at a heating rate of 2 K/min is significant when structural movements with characteristic times corresponding to frequencies between 0.1 to 10 Hz become thermally activated. Future work is needed in order to assess quantitatively the relationship between the degree of aging and the internal friction response of metallic glasses. The model presented here can

be used to estimate the loss modulus at low temperatures and frequencies below the attainable experimental window of conventional DMA measurements and, therefore, it may be used for studying the relationship between the intrinsic relaxation processes of the material and the activation of physical aging at lower temperatures and longer annealing times.

The relaxed state (red line in figure 1) of $Pd_{42.5}Ni_{7.5}Cu_{30}P_{20}$ still shows a significant amount of low temperature internal friction, as noticed by the prominent loss modulus shoulder. This is not the case in other metallic glasses in which well relaxed states only show a low-temperature excess wing of the primary relaxation[9,17,34]. The presence of sub-T_g mechanical relaxation with significant intensity is found in most Pd-based metallic glasses and it is probably related to the good ductility shown by this family of amorphous metals[36]. The model developed here can be used to estimate the intensity of the mechanical relaxation processes at low frequencies, this giving information on the slow processes involved in the plastic deformation of metallic glasses.

The model presented is based on the following main simplifications: 1) The unrelaxed storage modulus M_0 is considered not dependent on temperature. Actually, M_0 is expected to decrease monotonically with temperature due to thermal expansion of the structure. The effect on the loss modulus (imaginary part) is small, as the work is focused on the loss modulus this effect has not been taken into account. In order to reproduce the experimental storage modulus this temperature dependence should be introduced in the model. 2) The primary relaxation is modeled by the one parameter CC-function. The symmetric CC function is not able to reproduce the high temperature region above the dynamic glass transition[8], here we adopted this simplification as the interest is focused on the sub-T_g

region. 3) The sub-T_g relaxation is assumed as consequence of just two processes. However, the broad relaxation secondary peak suggests a contribution of different processes covering a wide range of relaxation times, as observed by direct spectrum analysis of strain or stress relaxation in other metallic glasses[37–41].

As shown in figures 3 and 6, in spite of these simplifications the model is able to describe the sub-T_g loss modulus with good agreement to the experimental data. Moreover, the analysis presented in this work permits to clearly visualize some of the main properties of the relaxation spectrum of Pd-based glasses. Contrary to other systems like La-based and Fe-based glasses, which show a well differentiated secondary peak, $Pd_{42.5}Ni_{7.5}Cu_{30}P_{20}$ glass shows a broad and blunt secondary peak that cannot be modeled neither by the Fourier transform of a stretched exponential nor by the commonly used HN and CC functions. The simplification considering just two relaxation processes permits to estimate the temperature behavior of the average relaxation times, $\tau_\alpha(T)$ and $\tau_\beta(T)$, and the corresponding activation energies as shown in figure 2. However, the broad shape of the Bergman function needed to model the secondary process suggests that, below T_g, the system presents a broad distribution of relaxation mechanisms. These relaxations become gradually activated as temperature increases and progressively transform the low temperature elastic solid into a viscous liquid above T_g. In fact, the activation of viscous flow is observed below the glass transition at the same temperatures at which the tail of α-relaxation starts contributing to the loss modulus.

Surprisingly, this broad distribution of relaxation processes shows average activation energies within a rather narrow range of 160-230 kJ/mol. All the detected relaxation processes, including the faster events responsible of the low temperature tail of the

secondary peak (at temperatures more than 100 K below T_g) as well as the slow primary relaxation responsible of viscous flow near T_g show activation energies within this range. This is in contradiction with the potential energy landscape view of a secondary process with much lower activation energy barrier than the primary relaxation[42,43].

In many previous analyses, the activation energies were calculated in the glassy state ($T < T_g$) for β-relaxation and in the liquid state ($T > T_g$) for α-relaxation. The analysis presented here shows that at the same temperature the two processes has to surpass energy barriers not too different. The picture that emerges is the following; at temperatures below but near glass transition there are thermal activated structural movements which allow the system to relax and eventually flow under an applied stress. Whether or not these movements are collective is dictated by the duration of the applied stress. Under short stress cycles, the structural movements do not have time to align in a collective response and they just generate internal friction while, under constant stress, they concatenate resulting in complete relaxation or viscous flow after a long time. However, the average energy barriers controlling the activation of both short and long structural movements are not too different. In order to further elucidate this point a direct spectrum analysis from quasi-static stress relaxation measurements is currently undertaken and will be presented in future work.

CONCLUSIONS

The sub-T_g mechanical relaxation spectrum of $Pd_{42.5}Ni_{7.5}Cu_{30}P_{20}$ metallic glass is characterized by the overlapping between secondary and primary relaxations. The experimental response at different temperatures and frequencies has been successfully modeled by considering two relaxation processes with average relaxation times $\tau_\alpha(T)$ and $\tau_\beta(T)$. The model assumes Arrhenius-like dependences below glass transition and a VFT-

type behavior in the equilibrated super-cooled liquid state. Viscosity measurements show that α-relaxation remains active within the $0.9T_g$-T_g region with apparent activation energy lower than in the equilibrated liquid above the calorimetric T_g, and not too higher than that of the secondary process. The application of the model may help estimating the relaxation spectrum at frequencies and temperatures not attainable by the usual mechanical spectroscopy techniques.

AUTHOR INFORMATION. **Corresponding author**

*Eloi Pineda; eloi.pineda@upc.edu; Tel. (34) 935 521 141

ACKNOWLEDGMENT

C. Liu thanks the experimental assistance and the fruitful discussions with Mr. M. Madinehei and Dr. P. Bruna. Work funded by MINECO, grant FIS2014-54734-P, and Generalitat de Catalunya, grant 2014SGR00581. C. Liu is supported by Generalitat de Catalunya, FI grant 2012FI_B00237. J.C. Qiao would like to thank the financial support by the National Natural Science Foundation of China (No. 51401192).

REFERENCES

(1) Angell, C. A.; Ngai, K. L.; McKenna, G. B.; McMillan, P. F.; Martin, S. W. Relaxation in Glassforming Liquids and Amorphous Solids. *J. Appl. Phys.* **2000**, *88* (6), 3113.

(2) Qiao, J.; Pelletier, J.-M.; Casalini, R. Relaxation of Bulk Metallic Glasses Studied by Mechanical Spectroscopy. *J. Phys. Chem. B* **2013**, *117* (43), 13658–13666.

(3) Qiao, J.; Casalini, R.; Pelletier, J.-M.; Kato, H. Characteristics of the Structural and Johari-Goldstein Relaxations in Pd-Based Metallic Glass-Forming Liquids. *J. Phys. Chem. B* **2014**, *118* (13), 3720–3730.

(4) Vogel, H. The Temperature Dependence Law of the Viscosity of Fluids. *Phys. ZEITSCHRIFT* **1921**, *22*, 645–646.

(5) Fulcher, G. S. Analysis of Recent Measurements of the Viscosity of Glasses. *J. Am. Ceram. Soc.* **1925**, *8* (6), 339–355.

(6) Fulcher, G. S. Analysis of Recent Measurements of the Viscosity of Glasses. II. *J. Am. Ceram. Soc.* **1925**, *8* (12), 789–794.

(7) Tammann, G.; Hesse, W. The Dependancy of Viscosity on Temperature in Hypothermic Liquids. *ZEITSCHRIFT FUR Anorg. UND Allg. CHEMIE* **1926**, *156* (4), 245–257.

(8) Qiao, J. C.; Pelletier, J. M. Dynamic Universal Characteristic of the Main (α) Relaxation in Bulk Metallic Glasses. *J. Alloys Compd.* **2014**, *589*, 263–270.

(9) Pineda, E.; Bruna, P.; Ruta, B.; Gonzalez-Silveira, M.; Crespo, D. Relaxation of Rapidly Quenched Metallic Glasses: Effect of the Relaxation State on the Slow Low Temperature Dynamics. *Acta Mater.* **2013**, *61* (8), 3002–3011.

(10) Wang, L.-M.; Liu, R.; Wang, W. H. Relaxation Time Dispersions in Glass Forming Metallic Liquids and Glasses. *J. Chem. Phys.* **2008**, *128* (16), 164503.

(11) Yu, H.-B.; Wang, W.-H.; Samwer, K. The Beta Relaxation in Metallic Glasses: An Overview. *Mater. TODAY* **2013**, *16* (5), 183–191.

(12) Yu, H. Bin; Samwer, K.; Wang, W. H.; Bai, H. Y. Chemical Influence on Beta-Relaxations and the Formation of Molecule-like Metallic Glasses. *Nat. Commun.* **2013**, *4*, 2204.

(13) Okumura, H.; Inoue, A.; Masumoto, T. Glass-Transition and Viscoelastic Behaviors of La55al25ni20 and La55al25cu20 Amorphous-Alloys. *Mater. Trans. JIM* **1991**, *32* (7), 593–598.

(14) Wang, Z.; Yu, H. B.; Wen, P.; Bai, H. Y.; Wang, W. H. Pronounced Slow Beta-Relaxation in La-Based Bulk Metallic Glasses. *J. PHYSICS-CONDENSED MATTER* **2011**, *23* (14), 142202.

(15) Qiao, J. C.; Pelletier, J. M. Dynamic Mechanical Analysis in La-Based Bulk Metallic Glasses: Secondary (beta) and Main (alpha) Relaxations. *J. Appl. Phys.* **2012**, *112* (8), 083528.

(16) Rosner, P.; Samwer, K.; Lunkenheimer, P. Indications for an ``excess Wing{''} in Metallic Glasses from the Mechanical Loss Modulus in Zr65Al7.5Cu27.5. *Europhys. Lett.* **2004**, *68* (2), 226–232.

(17) Liu, C.; Pineda, E.; Crespo, D. Characterization of Mechanical Relaxation in a Cu–Zr–Al Metallic Glass. *J. Alloys Compd.* **2015**, *643*, S17–S21.

(18) Qiao, J. C.; Pelletier, J. M. Kinetics of Structural Relaxation in Bulk Metallic Glasses by Mechanical Spectroscopy: Determination of the Stretching Parameter βKWW. *Intermetallics* **2012**, *28*, 40–44.

(19) Khonik, V. A.; Ohta, M.; Kitagawa, K. Heating Rate Dependence of the Shear Viscosity of a Finemet Glassy Alloy. *Scr. Mater.* **2001**, *45* (12), 1393–1400.

(20) Csach, K.; Bobrov, O. P.; Khonik, V. A.; Lyakhov, S. A.; Kitagawa, K. Relationship between the Shear Viscosity and Heating Rate of Metallic Glasses below T G. *Phys. Rev. B* **2006**, *73* (9), 092107.

(21) Wang, Q.; Pelletier, J. M.; Xia, L.; Xu, H.; Dong, Y. D. The Viscoelastic Properties of Bulk Zr55Cu25Ni5Al10Nb5 Metallic Glass. *J. Alloys Compd.* **2006**, *413* (1-2), 181–187.

(22) Lee, M. L.; Li, Y.; Feng, Y. P.; Carter, W. C. Frequency-Dependent Complex Modulus at the Glass Transition in Pd 40 Ni 10 Cu 30 P 20 Bulk Amorphous Alloys. *Phys. Rev. B* **2003**, *67* (13), 132201.

(23) Liu, C. Dynamics of Metallic Glasses Explored by Mechanical Relaxation, Universitat Politècnica Catalunya - BarcelonaTech, 2015.

(24) Qiao, J. C.; Pelletier, J. M. Dynamic Mechanical Relaxation in Bulk Metallic Glasses: A Review. *J. Mater. Sci. Technol.* **2014**, *30* (6), 523–545.

(25) Hodge, I. M. Effects of Annealing and Prior History on Enthalpy Relaxation in Glassy-Polymers .6. Adam-Gibbs Formulation of Nonlinearity. *Macromolecules* **1987**, *20* (11), 2897–2908.

(26) Casalini, R.; Roland, C. M. Aging of the Secondary Relaxation to Probe Structural Relaxation in the Glassy State. *Phys. Rev. Lett.* **2009**, *102* (3), 035701.

(27) Taub, A. I.; Spaepen, F. The Kinetics of Structural Relaxation of a Metallic-Glass. *Acta Metall.* **1980**, *28* (12), 1781–1788.

(28) Spaepen, F. Homogeneous Flow of Metallic Glasses: A Free Volume Perspective. *Scr. Mater.* **2006**, *54* (3), 363–367.

(29) Böhmer, R.; Ngai, K. L.; Angell, C. A.; Plazek, D. J. Nonexponential Relaxations in Strong and Fragile Glass Formers. *J. Chem. Phys.* **1993**, *99* (5), 4201.

(30) Fan, G. J.; Fecht, H.-J.; Lavernia, E. J. Viscous Flow of the Pd43Ni10Cu27P20 Bulk Metallic Glass-Forming Liquid. *Appl. Phys. Lett.* **2004**, *84* (4), 487.

(31) Cole, K. S.; Cole, R. H. Dispersion and Absorption in Dielectrics I. Alternating Current Characteristics. *J. Chem. Phys.* **1941**, *9* (4), 341.

(32) Havriliak, S.; Negami, S. A Complex Plane Representation of Dielectric and Mechanical Relaxation Processes in Some Polymers. *Polymer (Guildf).* **1967**, *8*, 161–210.

(33) Svanberg, C. Correlation Function for Relaxations in Disordered Materials. *J. Appl. Phys.* **2003**, *94* (6), 4191–4197.

(34) Liu, C.; Pineda, E.; Crespo, D. Mechanical Relaxation of Metallic Glasses: An Overview of Experimental Data and Theoretical Models. *Metals (Basel).* **2015**, *5* (2), 1073–1111.

(35) Bergman, R. General Susceptibility Functions for Relaxations in Disordered Systems. *J. Appl. Phys.* **2000**, *88* (3), 1356.

(36) Wang, W. H. Correlation between Relaxations and Plastic Deformation, and Elastic Model of Flow in Metallic Glasses and Glass-Forming Liquids. *J. Appl. Phys.* **2011**, *110* (5), 053521.

(37) Kuršumović, A.; Scott, M. G.; Cahn, R. W. Creep Recovery Spectra in Fe40Ni40B20 Metallic Glass. *Scr. Metall. Mater.* **1990**, *24* (7), 1307–1312.

(38) Kuršumović, A.; Cantor, B. Anelastic Crossover and Creep Recovery Spectra in Fe40Ni40B20 Metallic Glass. *Scr. Mater.* **1996**, *34* (11), 1655–1660.

(39) Ocelík, V.; Csach, K.; Kasardová, A.; Bengus, V. Z. Anelastic Deformation Processes in Metallic Glasses and Activation Energy Spectrum Model. *Mater. Sci. Eng. A* **1997**, *226-228*, 851–855.

(40) Ju, J. D.; Jang, D.; Nwankpa, A.; Atzmon, M. An Atomically Quantized Hierarchy of Shear Transformation Zones in a Metallic Glass. *J. Appl. Phys.* **2011**, *109* (5), 053522.

(41) Ju, J. D.; Atzmon, M. A Comprehensive Atomistic Analysis of the Experimental Dynamic-Mechanical Response of a Metallic Glass. *Acta Mater.* **2014**, *74*, 183–188.

(42) Hachenberg, J.; Samwer, K. Indications for a Slow Beta-Relaxation in a Fragile Metallic Glass. *J. Non. Cryst. Solids* **2006**, *352* (42-49, SI), 5110–5113.

(43) Mayr, S. G. Relaxation Kinetics and Mechanical Stability of Metallic Glasses and Supercooled Melts. *Phys. Rev. B* **2009**, *79* (6), 060201.

TOC GRAPHIC